Author/s:
Huang, T;Holden, JA;Reynolds, EC;Heath, DE;O'Brien-Simpson, NM;O'Connor, AJ

Title:
Multifunctional Antimicrobial Polypeptide-Selenium Nanoparticles Combat Drug-Resistant Bacteria

Date:
2020-12-16

Citation:
Huang, T., Holden, J. A., Reynolds, E. C., Heath, D. E., O'Brien-Simpson, N. M. & O'Connor, A. J. (2020). Multifunctional Antimicrobial Polypeptide-Selenium Nanoparticles Combat Drug-Resistant Bacteria. ACS Applied Materials and Interfaces, 12 (50), pp.55696-55709. https://doi.org/10.1021/acsami.0c17550.

Persistent Link:
https://hdl.handle.net/11343/339583

Multifunctional antimicrobial polypeptide-selenium nanoparticles combat drug resistant bacteria

Tao Huang[1,2], James A. Holden[2], Eric C. Reynolds[2], Daniel E. Heath[1], Neil M. O'Brien-Simpson[2], and Andrea J. O'Connor[1,*]

[1] Department of Biomedical Engineering, University of Melbourne, Parkville, VIC 3010, Australia.

[2] Melbourne Dental School and The Bio21 Institute of Molecular Science and Biotechnology, The University of Melbourne, Parkville, VIC 3010, Australia.

* corresponding author; a.oconnor@unimelb.edu.au

ABSTRACT

Antibiotic-resistant bacteria are a severe threat to human health. The World Health Organisation's Global Antimicrobial Surveillance System has revealed widespread occurrence of antibiotic resistance among half a million patients across 22 countries, with *S. aureus*, *E. coli*, and *K. pneumoniae* being the most common resistant species. Antimicrobial nanoparticles are emerging as a promising alternative to antibiotics in the fight against antimicrobial resistance. In this work, selenium nanoparticles coated with the antimicrobial polypeptide, ε-poly-L-lysine, (Se NP-ε-PL) were synthesized and their antibacterial activity and cytotoxicity were investigated. The Se NP-ε-PL exhibited significantly greater antibacterial activity against all eight bacterial species tested, including Gram-positive, Gram-negative and drug-resistant strains, than their individual components, Se NP and ε-PL. The nanoparticles showed no toxicity towards human dermal fibroblasts at the minimum inhibitory concentrations, demonstrating a therapeutic window. Furthermore, unlike the conventional antibiotic kanamycin, the Se NP-ε-PL did not readily induce resistance in *E. coli* or *S. aureus*. Specifically, *S. aureus* began to develop resistance to kanamycin from ~44 generations, whereas it took ~132 generations for resistance to develop to the Se NP-ε-PL. Startlingly, *E. coli* was not able to develop resistance to the nanoparticles over ~300 generations. These results indicate that the multifunctional approach of combining Se NP with ε-PL to form Se NP-ε-PL is a highly efficacious new strategy with wide-spectrum antibacterial activity, low cytotoxicity, and significant delays in development of resistance.

KEYWORDS: *inorganic nanoparticle, antimicrobial peptide, cytotoxicity, antibacterial mechanism, antimicrobial resistance*

INTRODUCTION

The misuse of antibiotics has contributed to the rapid development of antibiotic-resistance,[1] which is currently recognised as a major challenge in the global healthcare systems.[2] A recent World Health Organisation report highlighted that the current and foreseeable conventional antibiotic pipeline is insufficient to meet the rise in antibiotic resistance.[3] Hence, new approaches to design and develop novel antibacterial agents are urgently needed.

Nanoparticles are promising non-drug antibacterial agents that offer an attractive alternative to antibiotics.[4] Silver nanoparticles (Ag NPs) have been the most extensively studied and used

antimicrobial nanoparticles, in part because they exhibited effective broad-spectrum antibacterial activity.[5] However, Ag NPs also showed toxicity to human cells and organs.[6-7] Recently, the antimicrobial activities of selenium nanoparticles (Se NPs) have attracted increased attention.[8] Unlike silver, selenium is a nutritional element in mammals.[9] It performs important roles in many biological activities, such as improving the immune responses to pathogens and viral antigens,[10-11] maintaining proper muscular function,[9] and preventing DNA oxidation.[12] Se NPs can be metabolized *in vivo*,[13] limiting potential accumulation in the body and long term toxicity, unlike many other nanoparticle systems. Further, Se NPs have been reported to exhibit significantly less toxicity towards human cells than other nanoparticles like Ag NPs.[14] Taken together, these properties make Se NPs promising antimicrobial agents for medical applications.

Se NPs demonstrated antibacterial activity predominantly against Gram-positive bacteria, including drug-resistant species such as methicillin-resistant *Staphylococcus aureus* (MRSA).[8, 15] However, most previously developed Se NPs showed little to no antibacterial activity against Gram-negative bacteria.[16] We have made multiple advances in the development of antibacterial Se NPs. By simply changing the size of polyvinyl alcohol (PVA) capped Se NPs, we were able to drastically reduce the minimum inhibitory concentration (MIC) and the minimum bactericidal concentration (MBC) of the particles, without significantly increasing their toxicity towards mammalian cells. Specifically, ~80 nm Se NPs exhibited the optimal antibacterial activity when compared to particles that were either smaller or larger.[8] We also extended antimicrobial activity of Se NPs to Gram-negative bacteria such as *E. coli* through capping the particles with a positively charged polymer (a recombinantly produced spider silk protein), likely due to stronger electrostatic interactions with the net-negative membrane of the Gram-negative bacteria.[16]

Engineering the surface chemistry of the Se NPs to provide antibacterial activity towards Gram-negative bacteria was a large advance. However, the utility of the spider silk recombinant protein capped Se NPs is limited due to problems with colloidal stability. while the spider silk recombinant protein capped Se NPs form stable suspension in water, they quickly precipitate in culture media. Thus, a new type of Se NP needs to be developed that provides effective broad-spectrum antibacterial activity, whilst retaining stability in physiological environments. Additionally, the recombinant spider silk protein has no inherent antibacterial activity. Using a positively charged antimicrobial peptide (AMP) as the capping layer has the potential to generate an Se NP system with broad spectrum antibacterial efficacy against both Gram-positive and Gram-negative species that is colloidally stable in physiological environments and further improve upon the antimicrobial activity by combining the inherent properties of Se NPs and AMPs.

AMPs are generally positively charged and have variable amino acid composition and length (from 6 to 100 residues).[17] The major antimicrobial mechanism of AMPs is disrupting the negatively charged bacterial cell membrane by virtue of their positive charge.[18] The antimicrobial activity of AMPs is concentration dependent, and the formation of stable pores in the bacterial membrane is only achieved when a certain concentration of AMPs bind to the bacterial membrane, named the “threshold point”.[19-20] However, high concentrations of free AMPs often exhibit high toxicity to mammalian cells.[21] Therefore, AMPs have had limited successful clinical translation to date. Developing technology that capitalises on the antibacterial activity of AMPs while minimising their toxicity towards mammalian cells will greatly enhance their therapeutic utility. A recent study found that the addition of Se NPs in a Se NP-lysozyme hybrid system could reduce the concentration of the AMP required to achieve

the same antibacterial efficacy.[22] However, this system still needed extremely high concentrations of both Se NPs and lysozyme to show antibacterial efficacy, and the most efficient nanohybrid system with 330 µg/mL Se NPs and 2000 µg/mL lysozyme, which may cause high levels of toxicity to mammalian cells, only showed 74% inhibition of *E. coli*. The antibacterial mechanism and cytotoxicity of this system were not elucidated in this work. Although coating with lysozyme increased the zeta potential of Se NPs, but the hybrid system still had a net negative charge, which may be one of the reasons why the system had a relatively low antibacterial efficacy.

The AMP ε-poly-L-lysine (ε-PL) was chosen in this work. ε-PL is composed of 25-30 L-lysine residues, and it is widely used as a food additive due to the broad spectrum antimicrobial activity.[23] ε-PL is also water soluble and exhibits low cytotoxicity.[24] Additionally, ε-PL generally has better antibacterial activity against Gram-negative bacteria than Gram-positive bacteria,[25] and we hypothesise that combining the complementary bactericidal properties of ε-PL and Se NPs is an attractive approach to create bespoke, broad spectrum antimicrobial agents.

In this contribution, we test the hypothesis that 80 nm Se NPs coated with ε-PL (Se NP-ε-PL) will exhibit improved colloidal stability and enhanced broad spectrum antimicrobial activity due to synergy between the Se NPs and the AMP capping layer, and that the effective dosage of the AMP can be reduced to limit potential toxicity. Additionally, we hypothesise that the ability of bacteria to develop resistance to these particles will be limited due to multimodal mechanisms of antibacterial action, and these hypotheses were confirmed by this study. The mechanism study and conclusion also provide insights into the design and fabrication of future antimicrobial materials that delay or prevent the development of resistance. Specifically, we developed these particles for use in wound care since the infection of chronic wounds is a significant and pressing challenge and the antioxidant and anti-inflammatory effects of selenium-based NPs are also very beneficial for wound healing.[26-27] However, these particles likely have a variety of other potential applications such as in anti-infective coatings on implantable devices.

RESULTS

Characterization of Se NP-ε-PL

The preparation process for the Se NP-ε-PL is shown schematically in Figure 1a. TEM images show spherical and highly monodispersed particles with diameters of approximately 80 nm (Figure 1b). These results are corroborated by the size distribution analysis that found a mean particle diameter of 82 nm and a polydispersity index of 0.055 (Figure 1c). ε-PL was adsorbed on the Se NPs surfaces electrostatically, resulting in an increase in the zeta potential of the Se NPs from a negative value of -7.2 ± 3.9 mV to a positive value of 13.2 ± 2.8 mV (Figure 1d,e). It was found that 0.96 ± 0.09 µg of ε-PL adsorbed per µg of Se NPs.

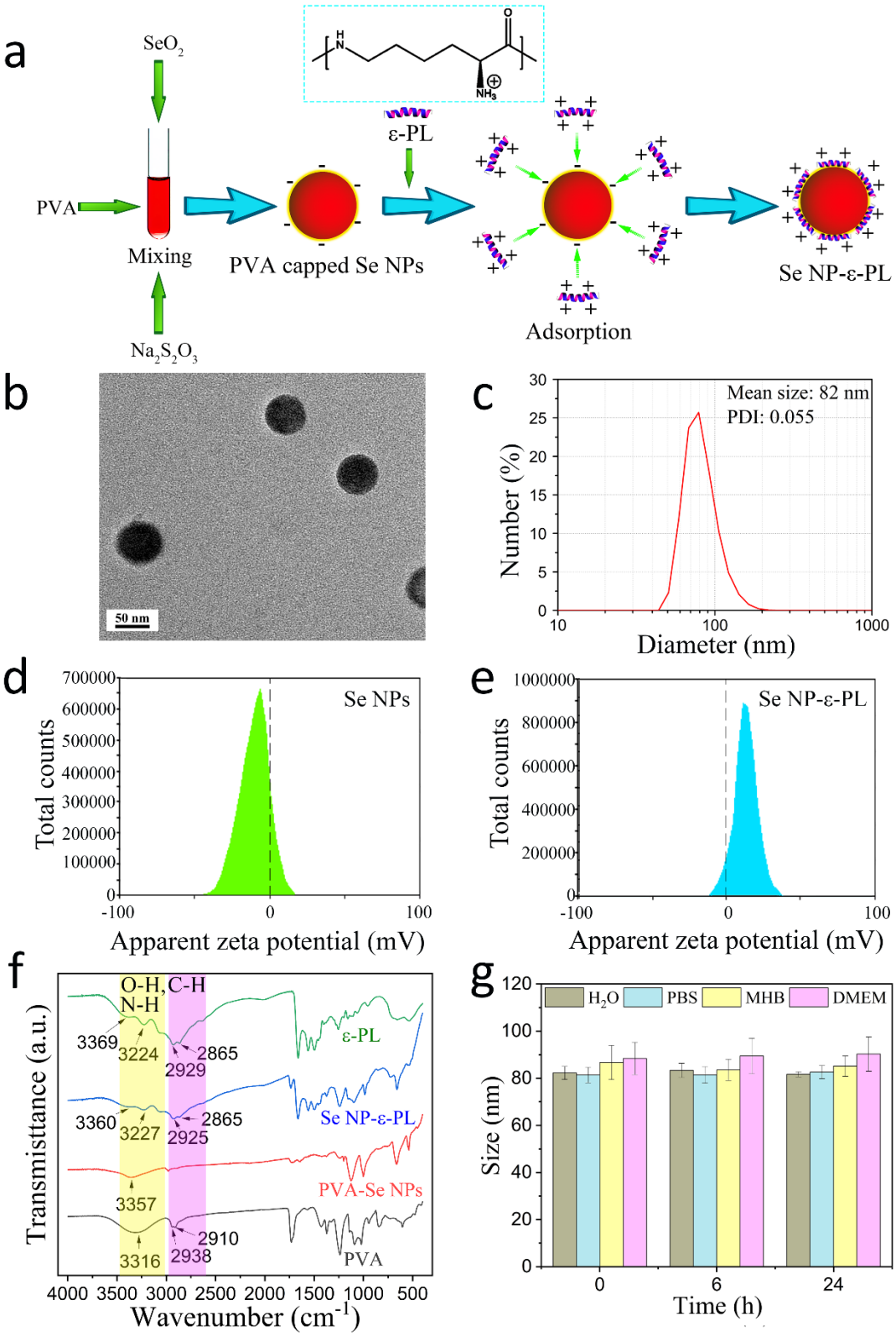

Figure 1. Characterization of Se NP-ε-PL. (a) Schematic illustration of the preparation of Se NP-ε-PL; (b) TEM image of Se NP-ε-PL (scale bar: 50 nm); (c) size distribution of Se NP-ε-PL measured by dynamic light scattering; (d), (e) representative zeta potential distributions of Se NPs and Se NP-ε-PL, respectively; (f) the FTIR spectra of PVA (grey curve), PVA capped Se NPs (red curve), Se NP-ε-PL (blue curve) and ε-PL (green curve); (g) the sizes of Se NP-ε-PL particles in different dispersants for time up to 24 h.

Fourier transform infrared (FTIR) was used to investigate the structural features of PVA capped Se NPs and Se NP-ε-PL in comparison to plain PVA and ε-PL (Figure 1f). Plain PVA showed a peak at 3316 cm^{-1} corresponding to O-H stretching vibrations. The peaks at 2938 cm^{-1} and 2910cm^{-1} correspond to C-H stretching from the alkyl groups. In comparison, PVA capped Se NPs showed a shift in the hydroxyl peak to 3357 cm^{-1}. This blue-shift indicated that PVA was conjugated to the surface of Se NPs through its -OH group.[8] In the spectrum of plain ε-PL, the peaks at 3369 cm^{-1} and 3224 cm^{-1} correspond to the primary and secondary amine stretching vibrations, respectively.[28-29] The peaks at 2929 and 2865 cm^{-1} are assigned to the symmetric and asymmetric C-H stretching vibrations.[28-29] The peaks in the ranges around 1690-1630 cm^{-1} and 1590-1480 cm^{-1} are associated with the vibrational modes of primary and secondary amide groups.[29] The Se NP-ε-PL showed a very similar spectrum to that of plain ε-PL, with just small shifts in the N-H and C-H peaks. These results suggest that ε-PL was physically adsorbed on the Se NPs.

The colloidal stability of the Se NP-ε-PL was tested through measuring the size of the particles after 0, 6 and 24 h in different dispersants, including ultra-pure water, phosphate buffered saline (PBS), Mueller Hinton broth (MHB) and complete Dulbecco's modified Eagle's medium (DMEM) (Figure 1g). The size of Se NP-ε-PL showed no significant difference after dispersing in these dispersants for different times, indicating that Se NP-ε-PL are colloidally stable in these four dispersants.

Se NP- ε-PL exhibit broad spectrum antimicrobial properties at significantly lower AMP concentrations

The abilities of the Se NPs, Se NP-ε-PL and pure ε-PL to inhibit the growth of bacteria were assessed. Firstly, treatment with Se NP-ε-PL was compared to using a simple blend of the equivalent amounts of Se NPs and free ε-PL (Se NPs + ε-PL) on *E. faecalis*, to investigate whether attaching the ε-PL to the Se NPs provided additional benefits. Both the MIC and MBC for the Se NP-ε-PL (9.4 ± 3.8 μg/mL and 23.2 ± 0.4 μg/mL, respectively) were found to be lower than those for the blend of Se NPs and free ε-PL (15.0 ± 1.6 μg/mL and 42.1 ± 3.7 μg/mL, respectively). This indicated that the Se NP-ε-PL did indeed show superior performance compared to a simple mixture of the two components toward at least some of the tested bacteria. Therefore, the antibacterial performance and mechanisms of action of the Se NP-ε-PL were then assessed on a range of types of bacteria.

The bacterial growth curves for eight types of bacteria in the presence of Se NPs, Se NP-ε-PL and pure ε-PL are presented in Figure S1 and Figure S2. The resulting MIC values for each antimicrobial agent are shown in Table 1. The Se NPs without ε-PL showed little or no effect on the growth of Gram-negative bacteria, as seen by the high MIC values (>200 μg/mL). However, significantly lower MICs were observed for Gram-positive strains (~10 μg/mL). These observations are consistent with previous findings that Se NP systems generally lack efficacy against Gram-negative strains.[16] In contrast, ε-PL alone had MIC values ranging from 7.5 to 27 μg/mL for all bacterial strains.

Table 1 The minimum inhibitory concentration (MIC) and minimal bactericidal concentration (MBC) values of Se NPs, Se NP-ε-PL and pure ε-PL against eight different strains of bacteria.

Strains	Gram	MIC (μg/mL)			MBC (μg/mL)		
		Se NPs	ε-PL	Se NP-ε-PL	Se NPs	ε-PL	Se NP-ε-PL
S.aureus	+	10.1 ± 6.6	7.5 ± 1.0	6.0 ± 0.3	35 ± 14	50.6 ± 3.5	17.5 ± 7.8
MRSA	+	11.5 ± 4.8	11.6 ± 2.0	8.6 ± 4.2	22.2 ± 2.0	149 ± 37	23.6 ± 1.0
E.faecalis	+	10.4 ± 5.8	27.1 ± 2.2	9.4 ± 3.8	119 ± 1	134 ± 10	23.2 ± 0.4
E.coli	-	340 ± 200[†]	13.2 ± 0.5	19.5 ± 9.2	1830 ± 830[‡]	24.3 ± 1.2	24.7 ± 0.6
A.baumannii	-	229 ± 10[†]	21.6 ± 7.0	13.8 ± 1.2	440 ± 290[‡]	50.0 ± 0.2	63 ± 17
P.aeruginosa	-	290 ± 66[†]	9.5 ± 3.6	12.5 ± 0.5	520 ± 290[‡]	25.0 ± 0.1	25.0± 0.2
K.pneumoniae	-	255 ± 29[†]	12.0 ± 0.6	12.3 ± 0.2	660 ± 310[‡]	12.9 ± 0.4	12.6 ± 0.1
K.pneumoniae (MDR)	-	363 ± 46[†]	26.5 ± 0.5	26.2 ± 0.4	1140 ±160[‡]	24.7 ± 0.5	25.0 ± 1.1

* All data are expressed as mean ± standard deviation (s.d.) of the biological replicates. [†] As Se NPs showed no total inhibition of growth of these bacteria within the tested concentrations, these MIC values calculated through linear fitting are only estimates for comparison. [‡] As Se NPs showed no total killing of these types of bacteria within the tested concentrations, these MBC values calculated through linear fitting are only estimates for comparison.

All the Gram-positive bacteria treated with Se NP-ε-PL had similar or lower MIC values compared to treatment with either component alone, potentially indicating cooperative action between the two components. The Gram-negative bacteria treated with Se NP-ε-PL exhibited an order of magnitude reduction in the MIC compared to Se NPs alone, illustrating that modifying the surfaces of Se NPs with cationic groups expanded the efficacy of Se NPs towards Gram-negative species.[16] The MIC values for Gram-negative strains treated with Se NP-ε-PL were similar to those for ε-PL alone. However, it is important to recognise that the Se NP-ε-PL particles contain approximately 50% ε-poly-L-lysine by weight. These results are significant because they allow for similar antibacterial properties to be obtained when using half the dose of the AMP. Such an advance could allow for the reduction in the amount of potentially toxic AMPs used in antibacterial treatments and could reduce the cost of such treatments by minimising the amount of the costly AMPs required.

The MBC values of the Se NPs, Se NP-ε-PL and ε-PL for the eight types of bacteria were determined via a colony forming unit assay. The results are shown in Figure S3 and Table 1. The colony forming unit (CFU) results showed that Se NPs had higher antibacterial activity against Gram-positive bacteria compared to ε-PL alone. In contrast, the ε-PL exhibited significantly better antibacterial activity against Gram-negative species in comparison to the Se NPs. However, only the combined Se NP-ε-PL showed strong antimicrobial properties against all eight types of bacteria tested. These results were confirmed through the MBC analysis. Coating the Se NPs with ε-PL resulted in markedly lower MBC values than for ε-PL alone and similar or lower values than for the Se NPs against the Gram-positive bacteria. Most prominently, Se NP-ε-PL had an MBC value that was approximately five times lower than the Se NPs or ε-PL alone against *E. faecalis*. When tested on Gram-negative bacteria, Se NP-ε-PL showed much lower MBC values than those for Se NPs and very similar values to those for pure ε-PL, despite the Se NP-ε-PL containing only half as much ε-PL.

Se NP-ε-PL use multiple mechanisms of action to kill bacteria

Four different potential mechanisms of action were assessed to investigate how the nanoparticles exert their antibacterial properties: Adenosine triphosphate (ATP) depletion, reactive oxygen species (ROS) generation, membrane depolarisation, and membrane disruption. *S. aureus* and *E. coli* were chosen as model Gram-positive and Gram-negative bacteria, respectively. *E. faecalis* was included because the Se NP- ε-PL showed a much higher bactericidal efficacy toward this type of bacteria than either Se NPs or ε-PL alone.

ATP is the intracellular energy source and plays a vital role in respiration, metabolism, and enzymatic reactions.[30] The depletion of cellular ATP in bacteria is a characteristic of energy-uncoupling effects, and would suggest a potential mechanism by which Se NP- ε-PL interfere with cellular metabolism.[31] Hence, the effects of Se NPs, Se NP-ε-PL and pure ε-PL on bacterial ATP level were investigated(Figure 2a-c). Se NPs showed greater ATP depletion activity than ε-PL in the Gram-positive bacteria *S. aureus* and *E. faecalis*, whereas ε-PL exhibited higher ATP depletion effects than Se NPs in the Gram-negative bacteria *E. coli*. However, the Se NP-ε-PL were as good or better at depleting ATP when compared to all other treatments for all tested bacteria.

The oxidative stress induced by high ROS production in response to nanoparticles is another important antibacterial mechanism.[32] Therefore, the effect of Se NPs, Se NP-ε-PL and pure ε-PL on bacterial ROS production were investigated (Figure 2d-f). Se NPs significantly increased the number of high ROS producing Gram-positive bacteria, *S. aureus* and *E. faecalis*, in a dose dependent manner. ε-PL exposure resulted in a slight increase in the number of high ROS producing Gram-negative bacteria *E. coli*, but not in that of the Gram-positive bacteria, *S. aureus* and *E. faecalis*. This may because Gram-negative bacteria are more sensitive to positively charged molecules than Gram-positive bacteria.[33] Se NP-ε-PL showed a moderate effect between those of Se NPs and ε-PL towards *S. aureus* and *E. faecalis*. For the Gram-negative bacteria *E. coli*, Se NP-ε-PL exposure resulted in the greatest percentage of high ROS producing cells, potentially indicating a cooperative effect between the nanoparticles and the ε-poly-$_{L}$-lysine coating.

Cell membrane depolarisation is another well-established mechanism of action of antimicrobial agents.[34] Therefore, the ability of the antimicrobial agents to depolarise the bacterial membranes was investigated (Figure 2g-i). Bacteria in pure MHB were used as the untreated control and bacteria treated with carbonyl cyanide chlorophenylhydrazone (CCCP, a standard depolarisation agent) were used as a depolarized control. Se NP exposure resulted in few cells with depolarised membranes. However, Se NP-ε-PL and pure ε-PL were able to depolarise the membranes of similar numbers of bacteria. Interestingly, CCCP is a standard depolarising agent, yet shows minimal activity towards *E. coli* in contrast to the Se NP-ε-PL which showed strong depolarisation activity.

Damage to the lipid bilayer of the bacterial membrane is another common mechanism of action that can result in bacterial death.[35] Bacteria with a damaged lipid bilayer will stain positive for propidium iodide (PI), indicating that exposure to an antibacterial agent disrupted their membrane.[20] The ability of our antimicrobial materials to disrupt bacterial membranes was assessed by quantifying the percentage of PI positive cells, and these data are presented in Figure 2j-l. Se NPs were the least effective at disrupting the bacterial membranes. However, Se NP-ε-PL and pure ε-PL showed significant membrane disruption effects for the three types of bacteria tested.

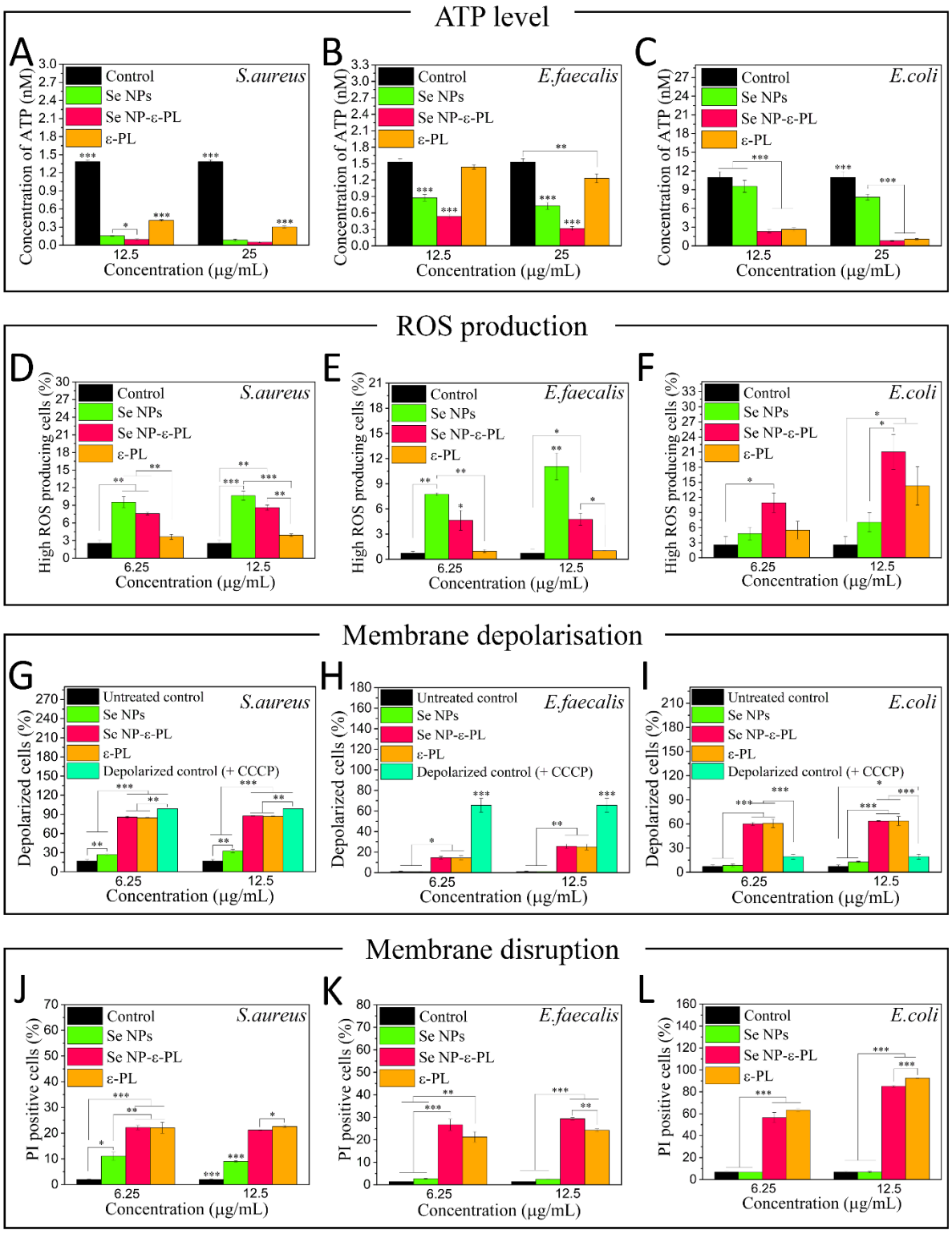

Figure 2. Investigation of antibacterial mechanisms: (a-c) ATP levels, (d-f) the percentage of cells that are producing high quantities of reactive oxygen species (ROS), (g-i) the percentage of cells that have a high degree of membrane depolarization, and (j-l) the percentage of propidium iodide (PI) positive bacterial cells of *S. aureus*, *E. faecalis* and *E. coli* treated with specified concentrations of Se NPs, Se NP-ε-PL or pure ε-PL, with bacteria in pure MHB as a control. One-way ANOVA analysis was adopted to compare means of experimental groups, * represents the P-value < 0.05, ** represents the P-value < 0.01 and *** represents the P-value < 0.001. The asterisk(s) directly marked on a bar indicate(s) this group is significantly different to all other groups treated at the same concentration.

In order to observe cytopathic effects, helium ion microscopy (HIM) was used to observe the bacterial morphology after treatment with Se NPs, Se NP-ε-PL or pure ε-PL, with bacteria in pure MHB as a control (Figure 3). The results corroborate the general trends in antibacterial activity seen in the other data presented herein. Specifically, the Gram-positive bacteria, *S. aureus* and *E. faecalis*, were damaged by all three antimicrobial treatments as seen through changes in cell shape and surface morphology. Many cells were also lysed, expelling their contents into the surrounding environment. Additionally, what appear to be Se NP-ε-PL attached to the bacteria was observed (pink arrows in Figure 3c,g).

Unlike the Gram-positive bacteria, significant cell damage was not observed for the Gram-negative bacteria treated with Se NPs. Additionally, few particles were found to adhere to surface of the *E. coli* and *K. pneumoniae* (Figure 3j,r); instead, many nanoparticles were observed in the environment surrounding these bacteria. These two bacteria have significantly higher negative surface charges than the other bacteria tested here (Table S1). Likely, the negatively charged Se NPs were unable to bind to the more negatively charged bacteria due to electrostatic repulsion. The Se NPs could still interact and attach to the surfaces of *A. baumannii* (Figure 3n) which has a lower negative zeta potential, similar to *S. aureus* and *E. faecalis*. (Table S1). However, as a Gram-negative bacterium, *A. baumannii* has a typical double lipid bilayer membrane system.[36] Even when Se NPs attach to the outer lipid bilayer of the bacteria, they may not be able to cross the periplasmic space and interact with the inner lipid bilayers. This may explain why these bacteria were not highly susceptible to damage by the Se NPs without ε-PL and showed relatively large MIC and MBC values. However, damage towards all Gram-negative bacteria species treated with either ε-PL or Se NP-ε-PL was observed. Additionally larger numbers of the Se NP-ε-PL particles were seen attaching to the Gram-negative bacteria, potentially due to more favorable electrostatic interactions (pink arrows in Figure 3k,o,s).

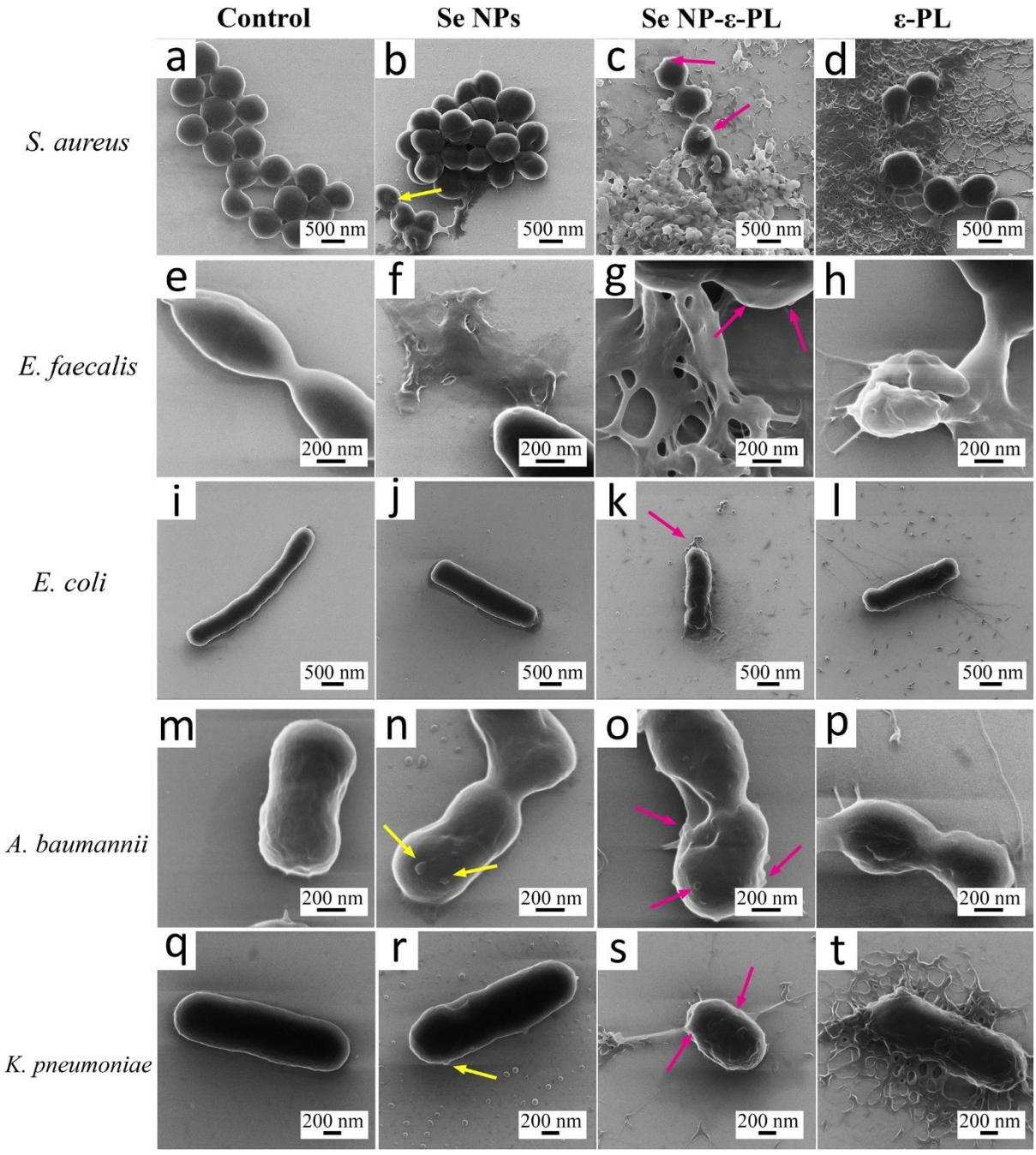

Figure 3. Helium ion microscopy images of bacteria. (a-d) *S. aureus*, (e-h) *E. faecalis*, (i-l) *E. coli*, (m-p) *A. baumannii* and (q-t) *K. pneumoniae* with Se NPs, Se NP-ε-PL or pure ε-PL, with bacteria in pure MHB as a control. Yellow and pink arrows indicate Se NPs and Se NP-ε-PL attached to the bacteria, respectively.

Resistance development assessment

The development of antimicrobial resistance is a significant healthcare challenge. Next generation antibacterial agents must be designed to limit or eliminate the development of future resistance. However, the development of resistance to nanoparticles remains largely unstudied.

In these experiments, the development of resistance in *S. aureus* to Se NPs and Se NP-ε-PL and *E. coli* to Se NP-ε-PL over 300+ generations was assessed to determine if we can generate a nanoparticle system that prevents or significantly delays the development of antimicrobial resistance. Resistance studies were not performed for *E. coli* to Se NPs as this bacterial strain is largely insensitive to this treatment. Kanamycin was used as a conventional antibiotic control. *S. aureus* began to develop resistance to kanamycin after only 44 generations (Figure 4a), as seen by the increase in the MBC value. Resistance towards nanoparticles was observed, but not until significantly longer exposure times. The onset of resistance in *S. aureus* to the Se NPs was observed at 110 generations and at 132 generations for the Se NP-ε-PL (Figure 4a). Interestingly, the fold change in MBC for *S. aureus* towards the Se NPs was very high (~50), while it remained at ~3.5 for both the antibiotic control and the Se NP-ε-PL. Startlingly, *E. coli* developed resistance to kanamycin at 52 generations; however, the bacteria were unable to develop resistance to the Se NP-ε-PL over the entire 312 generations tested (Figure 4b). This data illustrates that bacteria do have the capacity to develop resistance to antimicrobial nanoparticles. However, if the particles are designed appropriately, the onset of resistance can be significantly limited and potentially eliminated.

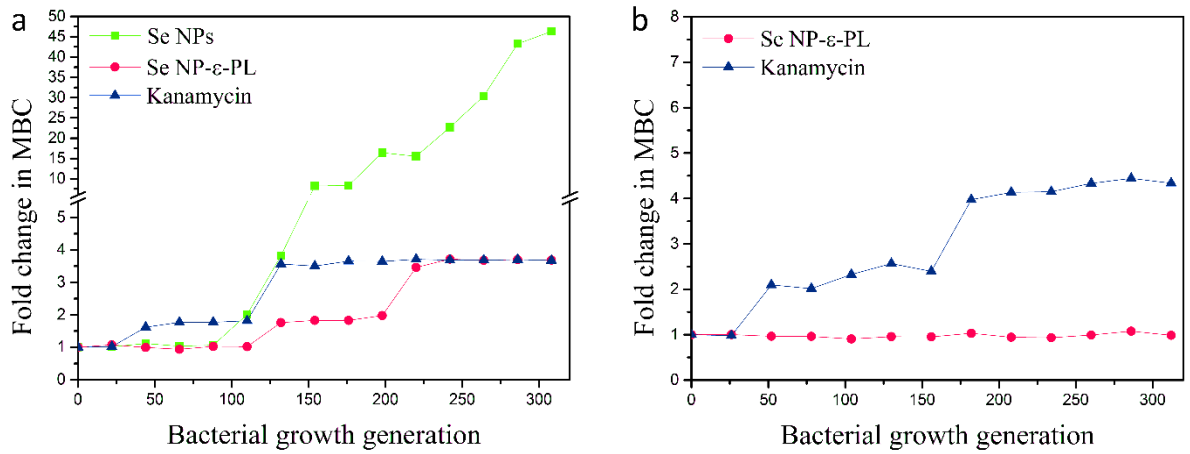

Figure 4. Resistance development (fold change in MBC). (a) Resistance development of *S. aureus* with Se NPs, Se NP-ε-PL or kanamycin; and (b) Resistance development of *E. coli* with Se NP-ε-PL or kanamycin.

Se NP-ε-PL do not exhibit cytotoxicity towards human dermal fibroblasts

In addition to exhibiting strong antibacterial properties, next generation antimicrobial agents must also exhibit cytocompatibility with mammalian cells at therapeutic doses. Since these particles were designed for use in the treatment of chronic wounds, human dermal fibroblasts were selected to illustrate the cytocompatibility of the particles. Specifically, the viabilities of human dermal fibroblasts (HDFs) after exposure to Se NPs, Se NP-ε-PL or pure ε-PL were assessed using an assay that measures the metabolic activity of the cells as a proxy for cell viability (Figure 5). The viability of HDFs after treatment with Se NPs at concentrations lower than or equal to 10 µg/mL showed no significant difference to that of the untreated control (Figure 5a). Se NP-ε-PL showed no significant cytotoxicity up to and including doses of 25 µg/mL (Figure 5b), while ε-PL treatment showed no cytotoxicity over the full range of

concentrations used in this study (Figure 5c). International Standard ISO 10993-5 describes assessment of *in vitro* cytotoxicity and states that reductions in viability of < 30% are not considered as toxic effects.[37] As such, the Se NPs at concentrations up to 25 µg/mL and Se NP-ε-PL up to 50 µg/mL were not classified as cytotoxic after 24 h of exposure. These results are corroborated by a lactase dehydrogenase (LDH) release assay, as shown in Figure S4.

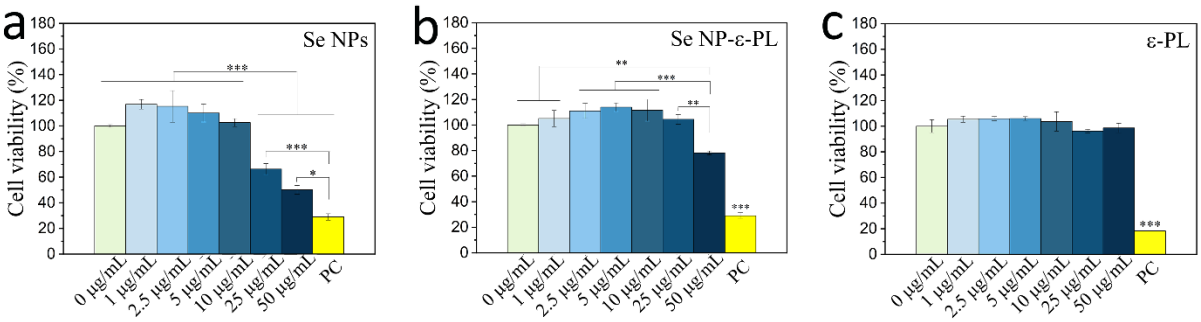

Figure 5. Viability of human dermal fibroblasts after 24 h exposure to different concentrations of (a) Se NPs, (b) Se NP-ε-PL and (c) pure ε-PL. PC is the positive control. A One-way ANOVA followed by Tukey's Post Hoc test was used to compare means of experimental groups, * p-value < 0.05, ** p-value < 0.01 and *** p-value < 0.001. The asterisk(s) directly marked on a bar indicate(s) this group is significantly different to all other groups.

DISCUSSION

Antibacterial efficacy and cytocompatibility of Se NP-ε-PL

Previously reported Se NPs showed relatively low antibacterial efficacy, with MIC values higher than 60 µg/mL against the common Gram-positive bacteria, *S. aureus*,[38-44] and even worse performance against Gram-negative bacteria, showing no significant effect[39, 43] or high MIC values: >100 µg/mL against *E. coli*[38, 42, 45] and *P. aeruginosa*[40, 42-43, 46] and >250 µg/mL against *K. pneumoniae*.[44, 46] In our previous work, ~80 nm PVA capped Se NPs were fabricated and showed strong antibacterial efficacy against *S. aureus* and MRSA, with MIC values of only 16 ± 7 µg/mL and 12 ± 2 µg/mL, respectively.[8] However, these NPs still had very weak antibacterial activity against Gram-negative bacteria. We developed positively charged Se NP by coating the particles with a positively charged recombinant spider silk protein and illustrated improved antibacterial activity against Gram-negative bacteria.[16] However, the poor colloidal stability of these Se NPs under physiological conditions significantly limits their potential medical applications. Additionally, assays done with similarly sized particles made fully of the recombinant spider silk did not show significant antimicrobial capacity. This data indicated that they positive surface charge enhanced the antimicrobial properties of the particles by improving electrostatic interactions between the particles and cells. However, the positive charges displayed by the spider silk were not antimicrobial in and of themselves. In the present work, Se NPs were coated with ε-PL through a simple adsorption step to create the positively charged Se NP-ε-PL system. These particles were superior to previous selenium-based antimicrobial nanoparticles in that they are colloidally stable in cell culture media, exhibit broad spectrum antimicrobial activity against Gram-positive, Gram-negative, and drug-

resistant bacteria, and the polycationic capping layer has inherent antimicrobial activity. Relatively low MIC values were found for the Se NP-ε-PL against the three Gram-positive bacteria strains tested (6.0-9.4 μg/mL) (Table 1). More significantly, for the five Gram-negative bacteria strains tested the MIC values for the Se NP-ε-PL were dramatically lower than those for the Se NPs without the ε-PL coating, with an order of magnitude lower dose required to reach the MIC (12.3-26.2 μg/mL). These results indicate that the Se NP-ε-PL system exhibits synergy for some bacteria (e.g., *E. faecalis*) compared to mixtures of free nanoparticles and AMP, and it is the only treatment with good broad-spectrum activity against all eight types of bacteria tested. Additionally, the antimicrobial activity of Se NP-ε-PL was comparable to or better than treatment with Se NPs alone or ε-PL alone. In addition to excellent antimicrobial activity, a successful antibacterial nanoparticle system requires mammalian cytocompatibility at therapeutic doses. The cytotoxicity results indicated that the safe concentration of Se NP-ε-PL is up to 50 μg/mL for HDFs, while the MICs of Se NP-ε-PL against the eight different types of bacteria tested are around 6 - 26 μg/mL, significantly lower than 50 μg/mL. With the exception of the MBC of Se NP-ε-PL against *A. baumannii* (63.0 ± 17.0 μg/mL), the MBCs of the Se NP-ε-PL to the different types of bacteria tested are around 13 - 25 μg/mL, also well below the level required to observe any cytotoxic effects. Notably, the viability assay was performed on HDFs after 24 h exposure to Se NP-ε-PL, while the antibacterial tests were performed only after 1.5 h exposure to Se NP-ε-PL, indicating the acute toxicity of Se NP-ε-PL towards the bacteria and the relatively benign interactions with the human cells at the tested concentrations. These results illustrate that the Se NP-ε-PL system has the potential to be a potent broad-spectrum antimicrobial material in medical applications.

Additionally, the Se NP-ε-PL system has many advantages when compared to other antimicrobial nanoparticle systems. Comparing to metallic nanomaterials such Ag-[5] and Au-NPs,[47] Se NPs are made from an essential trace element and show much lower toxicity toward mammalian cells.[14] Moreover, Se NPs can be metabolized and excreted through urine, allowing for eventual removal from the body.[13] In contrast, the silver and gold are not a part of the body's elemental composition and are relatively stable and long lasting in the body.[48-49] Numerous types of metal oxide NPs have also been explored for antibacterial applications, such as ZnO NPs[50], TiO_2 NPs[51] and CuO NPs.[52] However, they generally exhibit high MIC and MBC values (> 100 μg/mL).[50-52]

Organic antibacterial nanomaterials have also shown promise; however, they are generally less stable than the inorganic antibacterial materials, especially at high temperatures and pressures.[53] The recently developed structurally nanoengineered antimicrobial peptide polymers (SNAPPs) exploit the interactions of positively charged peptide components with Gram-negative bacteria, similarly to this work. They showed antibacterial effects against Gram-negative bacteria both *in vitro* and *in vivo*.[54] However, their MBC values were higher than the Se NP-ε-PL developed here, with MBC values against *E. coli*, *P. aeruginosa* and *K. pneumoniae* of 31.5 ± 2.6, 62.2 ± 3.5 and 67.5 ± 3.5 μg/mL, respectively.

It is important to note that dissolved biomolecules such as serum proteins may adsorb onto the surface of antibacterial nanoparticles *in vitro* or *in vivo*. This adsorbed protein layers, known as a biocorona, may impact the antibacterial efficacy and cytocompatibility of these particles.[55-56] Future work will focus on assessing the performance of these nanomaterials in more physiologically relevant *in vitro* and *in vivo* systems. However, it is important to note that Se NP systems (without AMP coatings) have been shown to retain significant antimicrobial activity in *in vivo* animal models.[57]

Se NP-ε-PL exert their antimicrobial effects via multiple mechanisms of action

The antimicrobial mechanisms identified for Se NP-ε-PL include ATP depletion, increased ROS production, membraned depolarisation, and membrane disruption, as illustrated in Figure 6. The four mechanistic assays performed in this work are well-established in the literature, and they have been shown to initiate a cascade of events that can lead to cell death. For instance, ATP is the main energy source of cells, and the depletion of ATP exerts a negative impact on many biological processes including cell division and membrane transport, leading to the loss of viability of bacteria.[58] Excessive ROS production can induce transposition of transcription factors; increase of cytoplasmic calcium concentration; and damage DNA, cell membranes and cell proteins, resulting in the death of bacterial cells.[59] The disruption of membranes causes damage to the physical and functional integrity of cells, leakage of cytosolic contents, and eventually cell death.[60] Depolarization of bacterial membranes can affect various cellular processes associated with bacterial viability since membrane potential plays an important role in regulating a wide range of bacterial physiology and behaviors, including ATP synthesis, pH homeostasis, membrane transport, motility, electrochemical communication, the spatial organization of the cytoskeleton and cell division.[61]

Additionally, Se NPs and ε-PL have been shown to exert antibacterial properties through other mechanisms not assessed here including damage to genetic material[62] and various cellular proteins.[63] It is likely that some of these additional mechanisms of action are occurring in this system also.

The improved antibacterial activity of the Se NP-ε-PL compared to Se NPs and ε-PL is likely due to the improved electrostatic interaction between the particles and bacteria and the complimentary mechanisms of action through which the nanoparticles and AMP exert their antibacterial activities. Much of the antibacterial activity of Ag NPs is thought to arise from the Ag ions shed from the particles.[64] In contrast, selenium is sparingly soluble in aqueous conditions.[65] As such, it is expected that physical contact between the particles and the bacteria is necessary to achieve their antibacterial activity. Generally, the surface potential of bacterial membranes is negative.[16] Changing the surface charge of the Se NPs to be positive through adsorption of the ε-PL enabled improved electrostatic interactions between the Se NP-ε-PL and the bacteria. This is best seen through the interaction of the particles with *E. coli* and *K. pneumoniae*, the bacteria with the largest negative surface charges (Table S1). The HIM images showed that the negatively charged Se NPs were largely unable to attach to the bacterial membranes (Figure 3). However, the positively charged Se NP-ε-PL particles were able to bind to the bacterial membranes (Figure 3).

Additionally, cooperative effects between the Se NPs and ε-PL were observed for the Se NP-ε-PL particles. This is best seen in the ATP depletion studies and the ROS production studies. In both assays, neither antibacterial agent alone was able to greatly impact all three of the tested bacteria. Only the Se NP-ε-PL system was able to significantly reduce ATP levels and promote ROS production for all three types of bacteria (Figure 2).

Furthermore, the Se NP-ε-PL particles showed strong antibacterial properties at significantly lower AMP concentrations. This is likely due to the local high concentration of AMP present at the particle interface. Membrane disruption models require a threshold concentration of AMP to be present before membrane disruption can occur.[19-20] By adsorbing the AMP molecules to the particle surface, regions of high AMP concentration are created, and these regions of local high density are likely able to disrupt the bacterial membrane, even when the bulk concentration of AMP is below the threshold point. This also explains why the Se NP-ε-

PL particles showed greater antibacterial properties compared to treatment with Se NPs and free ε-PL. This mechanism is similar to that hypothesised for the structurally nanoengineered antimicrobial peptide polymers (SNAPPs). The SNAPPs are star polymers with either 16 or 32 arms, and it is believed that their strong antibacterial properties arise due to the multivalence of AMPs that acts to increase their local concentration.[54]

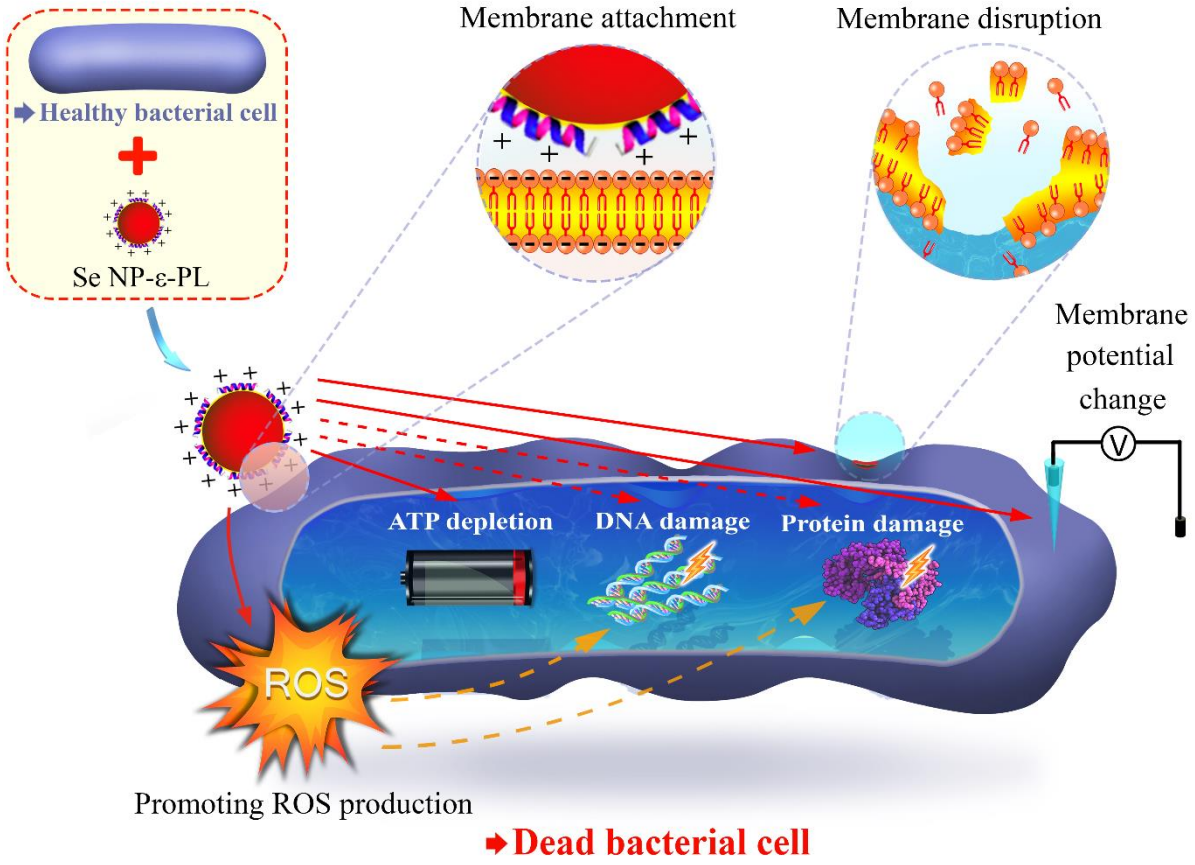

Figure 6. Schematic of the hypothesized antibacterial mechanism of Se NP-ε-PL. The Se NP-ε-PL can attach to the bacterial cell membrane through electrostatic interactions. The Se NP-ε-PL will then damage bacterial cell through promoting ROS production, depleting ATP, changing membrane potential and disrupting the membrane (indicated by red solid arrows). The Se NP-ε-PL has the potential to induce DNA damage and protein damage as well (indicated by red dashed arrows).[62-63] Additionally, the excessive amount of ROS can also induce damage of DNA and protein[59] (indicated by yellow dashed arrows).

Bacterial resistance

The development of bacterial resistance to nanoparticles is generally considered less likely than to conventional antibiotics because nanoparticles can kill bacteria through multiple mechanisms of action.[4] Therefore, the multiple antibacterial mechanisms of Se NP-ε-PL are expected to limit the development of antimicrobial resistance in comparison to many antibiotics that have only a single antibacterial mechanism. To illustrate this, kanamycin was selected as the antibiotic control in this work. Kanamycin exerts its antibacterial properties through a single mechanism, interfering with protein synthesis by binding to the bacterial ribosome.

During the long-term resistance assays, *S. aureus* and *E. coli* were able to rapidly develop resistance to kanamycin, after only 44 and 52 generations, respectively. In contrast, *S. aureus* developed resistance to the Se NP-ε-PL particles until 132 generations and the *E. coli* failed to develop resistance over the entire 312 generations of the assay. Interestingly, *S. aureus* developed resistance to the PVA-capped Se NPs at an earlier timepoint, 110 generations. These results support the theory that designing bespoke antimicrobial agents that leverage a larger number of antimicrobial mechanisms can limit the future development of resistance. Beyond the development of the next generation Se NP-ε-PL particles presented in this study, these results also elucidate fundamental design criteria for the creation of future antibacterial agents. Particularly, this work illustrates that designing particle-bacterial membrane interactions can be key towards improving antibacterial activity of particles and that appropriate layering of antimicrobial mechanisms can delay – and potentially eliminate – the development of resistance.

In general, the development of bacterial resistance to nanoparticles is largely unexplored. What work has been done has almost extensively focused on Ag NPs[64] and Au NPs.[66] It was shown that bacteria could develop resistance to Ag NPs through the production of the flagellin protein that causes aggregation of Ag NPs and reduces their antibacterial activity.[64] Additionally, researchers have reported that *E. coli* can develop resistance to Au NPs after only 21 generations, though the mechanism remains unknown.[66]

The authors are not aware of any previous reports on the development of resistance to selenium nanoparticle systems. The present work demonstrated that *S. aureus* can develop resistance to Se NP-ε-PL particles. However, significantly longer times were needed for the bacteria to acquire resistance in comparison to an antibiotic control and the Au NPs previously reported.[66] Startlingly, *E. coli* failed to develop resistance to the Se NP-ε-PL particles after more than 300 population doublings (24 days of culture). In contrast, two strains of *E. coli* were previously reported to develop resistance to Ag NPs after 6 and 13 days of culture, respectively.[64] These results may indicate that bacteria are less likely to develop resistance to Se NP-ε-PL than to Ag NPs and Au NPs. However, the different strains of bacteria and the different concentrations of NPs used in the long-term assays can affect the development of resistance limiting the conclusions that can be drawn through comparing these studies.

CONCLUSION

In this work, Se NP-ε-PL were fabricated, and their cytotoxicity and antibacterial activity were assessed. Se NP-ε-PL exhibited highly effective antibacterial activities on all eight different species of bacteria tested, including some drug-resistant strains. Considering antibacterial efficacy on both Gram-positive and Gram-negative bacteria, Se NP-ε-PL was found to be superior to both Se NPs alone and ε-PL alone. It was further demonstrated that bacteria are much less likely to develop resistance to Se NP-ε-PL than to traditional antibiotics for the two common strains tested, including *S. aureus* and *E. coli*. The efficient and wide-spectrum antibacterial activity of Se NP-ε-PL, low cytotoxicity, and low propensity to develop resistance in bacteria demonstrate the potential of Se NP-ε-PL to become a valuable new type of antibacterial agent.

METHODS

The synthesis of Se NPs and Se NP-ε-PL

Chemical reduction was used to fabricate Se NPs from SeO_2 with $Na_2S_2O_3$ as the reducing agent and PVA as the stabilising agent. PVA was dissolved in water at 10 mg/mL and SeO_2 was added to a final concentration of 5 mM. A separate solution of $Na_2S_2O_3$ in water was made at 0.4 M and 10 mL of this solution was added to 10 mL of the PVA/SeO_2 solution under magnetic stirring. After 2 h of reaction, the solution was immediately transferred to 1.7 mL Eppendorf tubes (1 mL per tube) and centrifuged at 15500 g for 10 min. The reaction liquid was replaced with water, and the Se NPs were redispersed using a vortex mixer. This rinsing procedure was repeated and then the Se NPs were redispersed in PBS and sterilized by filtering through 0.22 µm Millex-GV (PVDF) filters (Merck, Massachusetts, USA).

For the preparation of Se NP-ε-PL, the sterilized Se NP solution (100 µg) was centrifuged at 15500 g for 10 min. and the PBS solution was removed. Then the Se NPs were redispersed in 1 mL of a filter-sterilized solution of 2 mg/mL ε-PL in water. After 8 h immersion in the peptide solution, the particles were separated by centrifugation at 15500 g for 10 min, resuspended in 1 mL sterilized PBS and stored at 4 °C until use.

Characterization of the nanoparticles

The Se NP-ε-PL were observed using transmission electron microscopy (TEM, TECNAI F20) with an accelerating voltage of 200 keV. The size distributions and zeta potentials of Se NP-ε-PL in water were measured by using Zetasizer (Malvern, ATA Scientific) at 25 °C, setting selenium as the material with a refractive index of 2.6 and an absorption of 0.5, and water as the dispersant with refractive index of 1.330, a viscosity of 0.8872 cP and a dielectric constant of 78.5.[67]

To measure the total Se concentration of the Se NP and Se NP-ε-PL suspensions, the particles were dissolved in nitric acid, and inductively coupled plasma-optical emission spectrometry (ICP-OES, Varian 720-ES) was used to determine the Se ion concentrations.

The concentration of ε-PL was determined as previously reported.[68] Briefly, 80 µL trypan blue (Gibco, UK) solution was added to 1.92 mL sample solution. After 1h incubation at 37 °C, the solution was centrifuged at 15500 g for 5 min. Then 1 mL of the supernatant was transferred to a cuvette, and its absorbance was recorded using a UV–visible spectrophotometer (Varian 50Bio) at wavelengths of 200 nm to 800 nm. A standard curve at the peak wavelength of 585 nm from 0 µg/mL to 20 µg/mL (Figure S5) was used to determine the ε-PL concentrations.

FTIR analysis of PVA, PVA capped Se NPs, Se NP-ε-PL and ε-PL in the range of 4000-800 cm^{-1} was conducted on a Tensor-II spectrometer (Bruker).

The colloidal stability of the Se NP-ε-PL in different dispersants was tested, namely, water, PBS, MHB and complete DMEM (DMEM with 10% foetal bovine serum (FBS), 100 U/mL penicillin and 100 µg/mL streptomycin). First, 100 µg/mL Se NP- ε-PL were dispersed in 1 mL of each dispersant for 0, 6 and 24 h at 37°C, then the particle suspensions were centrifuged at 15500 g for 10 min. The dispersants were removed, and the Se NP- ε-PL were gently washed three times with water, then redispersed into water. Finally, the sizes of these particles were measured using Zetasizer (Malvern, ATA Scientific) at 37 °C, setting selenium as the material and water as the dispersant.

Antibacterial tests

Two different methods were used to test the antibacterial activity of Se nanoparticles: bacterial growth inhibition and a CFU assay. The methods used to determine the MIC and MBC used a plate microdilution method based on the CLSI 2015 guidelines M07[69] and M26[70], respectively as detailed below. Two independent experiments were performed.

Bacterial growth inhibition test. The bacterial strains methicillin-sensitive *Staphylococcus aureus* (*S. aureus*) ATCC 29213, methicillin-resistant *S. aureus* (MRSA) ATCC 43300, *Enterococcus faecalis* (*E. faecalis*) ATCC 29212, *Escherichia coli* (*E. coli*) ATCC 25922, *Acinetobacter baumannii* (*A. baumannii*) 2208 ATCC19606 , *Pseudomonas aeruginosa* (*P. aeruginosa*) strain PAO1-LAC ATCC 47085, *Klebsiella pneumoniae* (*K. pneumoniae*) ATCC 13883 and clinically isolated strain *K. pneumoniae* (MDR) FADDI-KP628, were obtained from the culture collection of The Melbourne Dental School, University of Melbourne, Australia. Bacteria were cultured in MHB at 37 °C. Serial two-fold dilutions of Se NPs, Se NP-ε-PL or pure ε-PL in 50 µL of PBS were added to each well of a 96-well microplate, followed by 50 µL of MHB with 2.5×10^6 bacteria/mL. The plate was put into an iEMS microplate reader (Pathtech Pty Ltd, Melbourne, Australia) at 37 °C to monitor bacterial growth by measuring the absorbance at a wavelength of 630 nm for 24 h. Background absorbance values due to the Se NP or Se NP-ε-PL solutions were subtracted from the measured values.

To calculate the MIC, the absorbance values of the bacteria growth curves at the time point when the stationary phase started (t_{sps}) were determined and calculated as a percentage of the untreated control ($Z=OD_a/OD_b\times100\%$, where OD_a is the absorbance of experimental groups and OD_b represents the absorbance of the negative control group, both at t_{sps} after subtraction of the culture medium background values). Then concentration-inhibition curves were plotted (Z vs. concentration), and a linear regression analysis used to determine the MIC at which Z becomes zero (Figure S6a).

CFU assay. Serial two-fold dilutions of Se NPs, Se NP-ε-PL or pure ε-PL in 50 µL of PBS were added into each well of 96-well microplates, followed by 50 µL MHB with 2.5×10^6 cells/mL bacteria. After incubating the microplate at 37 °C for 90 min., the bacterial solutions were diluted to 10^{-1}, 10^{-2}, 10^{-3} and 10^{-4} times, then 10 µL of each solution was transferred onto agar plates. The agar plates were incubated overnight, then the bacterial colony forming units were counted.

To calculate the MBC, concentration-killing curves were plotted with CFUs/mL as a function of antibacterial agent concentration, and linear regression analysis was used to estimate the lowest concentration (MBC) at which the CFU/mL would be zero (Figure S6b).

Antibacterial mechanism tests

In order to investigate the possible mechanisms of action of the nanoparticles on examples of Gram-positive and Gram-negative bacteria, the selected bacterial strains were each cultured in MHB at 37 °C. Serial two-fold dilutions of Se NPs, Se NP-ε-PL or pure ε-PL in 50 µL of PBS were added into the wells of 96-well microplates followed by 50 µL MHB with 2.5×10^6 cells/mL of the selected bacteria. 50 µL MHB with 2.5×10^6 cells/mL bacteria added to 50 µL PBS acted as the untreated control for the different tests described below.

ATP tests. To assess the levels of ATP in the bacteria, a set of the 96-well microplates was incubated for 1 h at 37 °C, then transferred to room temperature for further 30 min incubation. 100 µL of BacTiter-Glo^{TM} reagent (Promega, Australia) was added into each well, then mixed on an orbital shaker and incubated for 5 min. The luminescence was recorded using a microplate reader (PerkinElmer 1420 Multilabel Counter VICTOR3). A standard curve was generated by measuring the luminescence of 10-fold serial dilutions of ATP from 1 µM to 10 pM in 100 µL MHB after mixing for 1 min with 100 µL of the BacTiter-Glo^{TM} reagent.

ROS production tests. ROS production levels were measured on a set of the 96-well microplates after 90 min. Incubation at 37 °C, by adding CellROX® Orange Reagent to each well to a final concentration of 750 nM. The cells were further incubated for 1 h, then the fluorescence from the CellROX® Orange Reagent was measured on FL-3 (red fluorescence channel) using a Cell Lab Quanta SC MPL flow cytometer (Beckman Coulter). Two independent experiments were done for this test, and two technical replicates were done in each independent experiment.

Membrane potential change tests. Membrane potential changes in the bacteria with three different treatments (prepared as above) were detected relative to the untreated control and a fully depolarized control using a BacLight Bacterial Membrane Potential Kit (Invitrogen). CCCP was added to the untreated control at a final concentration of 5 µM as the fully depolarized control. 3,3‘-diethyloxacarbocyanine iodide ($DiOC_2(3)$) was added to all wells at a final concentration of 3mM. The $DiOC_2(3)$ exhibits green fluorescence in all bacterial cells when it is at low concentrations, but it will be more concentrated in healthy bacterial cells that maintain their membrane potential, and the fluorescence at the higher concentration shifts to be red. After 1h of incubation at 37 °C, the extent of depolarization of the cell membranes was assessed using a Cell Lab Quanta SC MPL flow cytometer (Beckman Coulter) to measure the ratio of cells that exhibited red fluorescence (FL-3) to those that displayed green fluorescence (FL-1). Gates were drawn based on the untreated (polarized) and CCCP-treated (fully depolarized) controls. Two independent experiments were done for this test, and two technical replicates were adopted for each independent experiment.

Membrane disruption tests. Disruption of the bacterial membranes was assessed after incubating the 96-well microplates for 90 min. At 37 °C. 0.1% of SYTO 9 and 0.1% of propidium iodide (PI) were added to each well and incubated again for 5 min. SYTO 9 is a green-fluorescent nucleic acid stain which can stain both live and dead Gram-positive and Gram-negative bacteria. PI is a red-florescent nuclear and chromosome counterstain but is not permeant to cells with intact plasma membranes. A Cell Lab Quanta SC MPL flow cytometer (Beckman Coulter) was used to measure the percent of PI-positive cells to show the fraction with increased membrane permeability.[20] Two independent tests were performed, and two parallel samples were used in each test for each variation.

HIM images. The morphologies of bacterial strains methicillin-sensitive *S. aureus*, *E. faecalis*, *E. coli*, *A. baumannii*, and *K. pneumoniae* after treatment with Se NPs, Se NP-ε-PL or pure ε-PL were observed using Helium Ion Microscopy (HIM, Zeiss, Germany). The samples for this assessment were prepared as follows. Firstly, 100 µL of PBS solution with 125 µg/mL Se NPs, Se NP-ε-PL or pure ε-PL was added to each well of 96-well microplates, with 100 µL pure PBS used as an untreated control. Then, 100 µL of MHB with 1.25×10^7 /mL bacteria was added to each well. After 90 min. incubation at 37 °C, 10 µL of both treated and untreated bacteria was dropped onto clean silicon wafers, then placed in an oven at 37 °C for 20 min. to dry. The dried samples were transferred to a 12-well plate, 2.5% glutaraldehyde was added to each well to fix the bacterial cells for 1 h, then gradient ethanol solutions (30%, 50%, 60%, 70%, 80%,

90%, 95% and 100%) were used for dehydration. The prepared samples were finally dried in a fume hood overnight before imaging.

Bacterial resistance tests

The ability of methicillin-sensitive *S. aureus* to develop resistance to Se NPs and Se NP-ε-PL and the ability of *E. coli* to develop resistance to Se NP-ε-PL over an extended period in culture were tested. Tests were also run using the antibiotic kanamycin for comparison. First, a single *S. aureus* or *E. coli* colony from an agar plate was inoculated into 20 mL MHB and cultured overnight at 37 °C. The bacteria suspensions were diluted to 2.5×10^6 cells/mL. Then Se NPs, Se NP-ε-PL or kanamycin was added into 10 mL of the bacteria suspensions and cultured for 24 h (~11 generations growth of *S. aureus* and ~13 generations of *E. coli*). Each of the antibacterial agents was added at its MBC50 (the concentration that kills 50% of the bacteria) for each bacterial strain. The number of generations, N, was calculated using **Equation (1)**.

$$N = Log_2(\frac{C}{2.5\times10^6}) \quad (1)$$

where N represents the number of generations and C represents the concentration of bacteria after 24 h culture (bacteria/mL).

These bacteria suspensions were diluted again to 2.5×10^6 cells/mL, and 10 mL of each of the diluted suspensions was treated with Se NPs, Se NP-ε-PL or kanamycin at MBC50 and cultured for 24 h. These steps were repeated daily until over 300 generations of growth had occurred. After every 48 h, a CFU assay was performed on the bacteria, and the MBCs of the antibacterial agents were calculated as described above and plotted as a function of the number of generations since the start of the experiment.

Cytotoxicity tests on human dermal fibroblasts

Cytotoxicity assays were performed as previously reported.[8] A brief description of the protocol can be found in the SI.

Statistical analysis

Data in this work are expressed as means ± standard deviation. Statistical analysis was performed by one-way analysis of variance (ANOVA) followed by Tukey's post hoc tests using SPSS 25.0 and p-values less than 0.05 were considered statistically significant.

ACKNOWLEDGEMENTS

The National Health and Medical Research Council (NHMRC) of Australia and Australian Research Council (ARC) are thanked for financial support over many years for the nanomaterials, peptide chemistry and chemical biology studies reported in the authors' laboratories. NMOS is the recipient of NHMRC funding (APP1142472, APP1158841, APP1185426), ARC funding (DP160101312, LE200100163), Cancer Council Victoria

funding (APP1163284) and Australian Dental Research Funding in antimicrobial materials and research is supported by the Centre for Oral Health Research at The Melbourne Dental School. JAH is the recipient of NHMRC funding (APP1185426) and Australian Dental Research Funding in antimicrobial materials and research is supported by the Centre for Oral Health Research at The Melbourne Dental School. AO, DH and NMOS are recipients of funding from The Acceleration Fund of the Department of Health and Human Services, Victoria, Australia. TH gratefully acknowledges the support of the University of Melbourne and an Australian Government Research Training Program Scholarship (Melbourne International Research Scholarship). The authors thank Babak Nasr for help with HIM imaging, the Bio21 Advanced Microscopy Facility (the University of Melbourne), and the Materials Characterization and Fabrication Platform (the University of Melbourne) for access to infrastructure and equipment.

REFERENCES

(1) Byarugaba, D. Antimicrobial resistance in developing countries and responsible risk factors. *Int. J. Antimicrob. Agents* **2004,** *24* (2), 105-110.
(2) Theuretzbacher, U. Global antibacterial resistance: The never-ending story. *J. Glob. Antimicrob. Resist.* **2013,** *1* (2), 63-69.
(3) World-Health-Organization. Antibacterial agents in clinical development: an analysis of the antibacterial clinical development pipeline. **2019**.
(4) Makvandi, P.; Wang, C. y.; Zare, E. N.; Borzacchiello, A.; Niu, L. n.; Tay, F. R. Metal‐based nanomaterials in biomedical applications: Antimicrobial activity and cytotoxicity aspects. *Adv. Funct. Mater.* **2020**, 1910021.
(5) Akter, M.; Sikder, M. T.; Rahman, M. M.; Ullah, A. A.; Hossain, K. F. B.; Banik, S.; Hosokawa, T.; Saito, T.; Kurasaki, M. A systematic review on silver nanoparticles-induced cytotoxicity: Physicochemical properties and perspectives. *Journal of advanced research* **2018,** *9*, 1-16.
(6) Kittler, S.; Greulich, C.; Diendorf, J.; Köller, M.; Epple, M. Toxicity of silver nanoparticles increases during storage because of slow dissolution under release of silver ions. *Chem. Mater* **2010,** *22* (16), 4548-4554.
(7) Kim, S.; Choi, J. E.; Choi, J.; Chung, K.-H.; Park, K.; Yi, J.; Ryu, D.-Y. Oxidative stress-dependent toxicity of silver nanoparticles in human hepatoma cells. *Toxicol. In Vitro* **2009,** *23* (6), 1076-1084.
(8) Huang, T.; Holden, J. A.; Heath, D. E.; O'Brien-Simpson, N. M.; O'Connor, A. J. Engineering highly effective antimicrobial selenium nanoparticles through control of particle size. *Nanoscale* **2019,** *11*, 14937-14951.
(9) Underwood, E. *Trace elements in human and animal nutrition*, Elsevier: 2012.
(10) Duntas, L. H. The evolving role of selenium in the treatment of Graves' disease and ophthalmopathy. *J. Thyroid Res.* **2012,** *2012*.
(11) Chaudhary, S.; Umar, A.; Mehta, S. Surface functionalized selenium nanoparticles for biomedical applications. *J. Biomed. Nanotechnol.* **2014,** *10* (10), 3004-3042.
(12) Wang, H.; Zhang, J.; Yu, H. Elemental selenium at nano size possesses lower toxicity without compromising the fundamental effect on selenoenzymes: comparison with selenomethionine in mice. *Free Radic. Biol. Med.* **2007,** *42*, DOI: 10.1016/j.freeradbiomed.2007.02.013.
(13) Loeschner, K.; Hadrup, N.; Hansen, M.; Pereira, S. A.; Gammelgaard, B.; Møller, L. H.; Mortensen, A.; Lam, H. R.; Larsen, E. H. Absorption, distribution, metabolism and excretion of selenium following oral administration of elemental selenium nanoparticles or selenite in rats. *Metallomics* **2014,** *6* (2), 330-337.

(14) Biswas, D. P.; O'Brien-Simpson, N. M.; Reynolds, E. C.; O'Connor, A. J.; Tran, P. A. Comparative study of novel in situ decorated porous chitosan-selenium scaffolds and porous chitosan-silver scaffolds towards antimicrobial wound dressing application. *J. Colloid Interface Sci.* **2018,** *515*, 78-91.
(15) Tran, P. A.; Webster, T. J. Selenium nanoparticles inhibit Staphylococcus aureus growth. *Int J Nanomedicine* **2011,** *6*, 1553-1558.
(16) Huang, T.; Kumari, S.; Herold, H.; Bargel, H.; Aigner, T. B.; Heath, D. E.; O'Brien-Simpson, N. M.; O'Connor, A. J.; Scheibel, T. Enhanced antibacterial activity of Se nanoparticles upon coating with recombinant spider silk protein eADF4(κ16). *Int. J. Nanomedicine* **2020,** *2020* (15), 4275-4288.
(17) Bulet, P.; Stöcklin, R.; Menin, L. Anti‐microbial peptides: from invertebrates to vertebrates. *Immunol. Rev.* **2004,** *198* (1), 169-184.
(18) Duclohier, H.; Molle, G.; Spach, G. Antimicrobial peptide magainin I from Xenopus skin forms anion-permeable channels in planar lipid bilayers. *Biophys. J.* **1989,** *56* (5), 1017-1021.
(19) Huang, H. W. Molecular mechanism of antimicrobial peptides: the origin of cooperativity. *Biochimica et Biophysica Acta (BBA)-Biomembranes* **2006,** *1758* (9), 1292-1302.
(20) O'Brien-Simpson, N. M.; Pantarat, N.; Attard, T. J.; Walsh, K. A.; Reynolds, E. C. A rapid and quantitative flow cytometry method for the analysis of membrane disruptive antimicrobial activity. *PLoS One* **2016,** *11* (3), e0151694.
(21) Hancock, R. E.; Sahl, H.-G. Antimicrobial and host-defense peptides as new anti-infective therapeutic strategies. *Nat. Biotechnol.* **2006,** *24* (12), 1551-1557.
(22) Vahdati, M.; Moghadam, T. T. Synthesis and characterization of Selenium nanoparticles-Lysozyme nanohybrid System with Synergistic Antibacterial properties. *Sci. Rep.* **2020,** *10* (1), 1-10.
(23) Geornaras, I.; Yoon, Y.; Belk, K.; Smith, G.; Sofos, J. Antimicrobial Activity of ε‐Polylysine against Escherichia coli O157: H7, Salmonella Typhimurium, and Listeria monocytogenes in Various Food Extracts. *J. Food Sci.* **2007,** *72* (8).
(24) Hiraki, J.; Ichikawa, T.; Ninomiya, S.-i.; Seki, H.; Uohama, K.; Seki, H.; Kimura, S.; Yanagimoto, Y.; Barnett, J. W. Use of ADME studies to confirm the safety of ε-polylysine as a preservative in food. *Regul. Toxicol. Pharmacol.* **2003,** *37* (2), 328-340.
(25) Hyldgaard, M.; Meyer, R. L.; Peng, M.; Hibberd, A. A.; Fischer, J.; Sigmundsson, A.; Mygind, T. Binary combination of epsilon-poly-l-lysine and isoeugenol affect progression of spoilage microbiota in fresh turkey meat, and delay onset of spoilage in Pseudomonas putida challenged meat. *Int. J. Food Microbiol.* **2015,** *215*, 131-142.
(26) Ather, S.; Harding, K.; Tate, S. Wound management and dressings. In *Advanced textiles for wound care*; Elsevier: 2019; pp 1-22.
(27) Malhotra, S.; Welling, M.; Mantri, S.; Desai, K. In vitro and in vivo antioxidant, cytotoxic, and anti‐chronic inflammatory arthritic effect of selenium nanoparticles. *Journal of Biomedical Materials Research Part B: Applied Biomaterials* **2016,** *104* (5), 993-1003.
(28) Razavi, R.; Tajik, H.; Moradi, M.; Molaei, R.; Ezati, P. Antimicrobial, microscopic and spectroscopic properties of cellulose paper coated with chitosan sol-gel solution formulated by epsilon-poly-l-lysine and its application in active food packaging. *Carbohydr. Res.* **2020,** *489*, 107912.
(29) Lv, J. M.; Meng, Y. C.; Shi, Y. G.; Li, Y. H.; Chen, J.; Sheng, F. Properties of epsilon‐polylysine • HCl/high‐methoxyl pectin polyelectrolyte complexes and their commercial application. *J. Food Process. Preserv.* **2020,** *44* (2), e14320.
(30) Mempin, R.; Tran, H.; Chen, C.; Gong, H.; Ho, K. K.; Lu, S. Release of extracellular ATP by bacteria during growth. *BMC Microbiol.* **2013,** *13* (1), 301.
(31) Lok, C.-N.; Ho, C.-M.; Chen, R.; He, Q.-Y.; Yu, W.-Y.; Sun, H.; Tam, P. K.-H.; Chiu, J.-F.; Che, C.-M. Silver nanoparticles: partial oxidation and antibacterial activities. *JBIC Journal of Biological Inorganic Chemistry* **2007,** *12* (4), 527-534.
(32) Li, Y.; Zhang, W.; Niu, J.; Chen, Y. Mechanism of photogenerated reactive oxygen species and correlation with the antibacterial properties of engineered metal-oxide nanoparticles. *ACS nano* **2012,** *6* (6), 5164-5173.

(33) F Sperandio, F.; Huang, Y.-Y.; R Hamblin, M. Antimicrobial photodynamic therapy to kill Gram-negative bacteria. *Recent patents on anti-infective drug discovery* **2013,** *8* (2), 108-120.
(34) Bionda, N.; Fleeman, R. M.; Shaw, L. N.; Cudic, P. Effect of Ester to Amide or N‐Methylamide Substitution on Bacterial Membrane Depolarization and Antibacterial Activity of Novel Cyclic Lipopeptides. *ChemMedChem* **2013,** *8* (8), 1394-1402.
(35) Ibrahim, H. R.; Sugimoto, Y.; Aoki, T. Ovotransferrin antimicrobial peptide (OTAP-92) kills bacteria through a membrane damage mechanism. *Biochimica et Biophysica Acta (BBA)-General Subjects* **2000,** *1523* (2-3), 196-205.
(36) Nikaido, H. Multidrug efflux pumps of gram-negative bacteria. *J. Bacteriol.* **1996,** *178* (20), 5853.
(37) ISO. 10993-5: Biological evaluation of medical devices. *Tests for in vitro cytotoxicity* **2009**.
(38) Guisbiers, G.; Wang, Q.; Khachatryan, E.; Mimun, L.; Mendoza-Cruz, R.; Larese-Casanova, P.; Webster, T.; Nash, K. Inhibition of E. coli and S. aureus with selenium nanoparticles synthesized by pulsed laser ablation in deionized water. *Int. J. Nanomedicine* **2016,** *11*, 3731.
(39) Tran, P. A.; O'Brien-Simpson, N.; Reynolds, E. C.; Pantarat, N.; Biswas, D. P.; O'Connor, A. J. Low cytotoxic trace element selenium nanoparticles and their differential antimicrobial properties against S. aureus and E. coli. *Nanotechnology* **2015,** *27* (4), 045101.
(40) Srivastava, N.; Mukhopadhyay, M. Green synthesis and structural characterization of selenium nanoparticles and assessment of their antimicrobial property. *Bioprocess Biosystems Eng.* **2015,** *38* (9), 1723-1730.
(41) Shakibaie, M.; Forootanfar, H.; Golkari, Y.; Mohammadi-Khorsand, T.; Shakibaie, M. R. Anti-biofilm activity of biogenic selenium nanoparticles and selenium dioxide against clinical isolates of Staphylococcus aureus, Pseudomonas aeruginosa, and Proteus mirabilis. *J. Trace Elem. Med Biol.* **2015,** *29*, 235-241.
(42) Zonaro, E.; Lampis, S.; Turner, R. J.; Qazi, S. J. S.; Vallini, G. Biogenic selenium and tellurium nanoparticles synthesized by environmental microbial isolates efficaciously inhibit bacterial planktonic cultures and biofilms. *Front. Microbiol.* **2015,** *6*, 584.
(43) Boroumand, S.; Safari, M.; Shaabani, E.; Shirzad, M.; Faridi-Majidi, R. Selenium nanoparticles: synthesis, characterization and study of their cytotoxicity, antioxidant and antibacterial activity. *Mater. Res. Express* **2019,** *6* (8), 0850d8.
(44) Stevanović, M.; Filipović, N.; Djurdjević, J.; Lukić, M.; Milenković, M.; Boccaccini, A. 45S5Bioglass®-based scaffolds coated with selenium nanoparticles or with poly (lactide-co-glycolide)/selenium particles: processing, evaluation and antibacterial activity. *Colloids Surf. B. Biointerfaces* **2015,** *132*, 208-215.
(45) Beladi, M.; Sepahi, A. A.; Mehrabian, S.; Esmaeili, A.; Sharifnia, F. Antibacterial activities of selenium and selenium nano-particles (products from Lactobacillus acidophilus) on nosocomial strains resistant to antibiotics. *J. Pure Appl. Microbiol.* **2015,** *9* (4), 2843-2852.
(46) Cremonini, E.; Zonaro, E.; Donini, M.; Lampis, S.; Boaretti, M.; Dusi, S.; Melotti, P.; Lleo, M. M.; Vallini, G. Biogenic selenium nanoparticles: characterization, antimicrobial activity and effects on human dendritic cells and fibroblasts. *Microb. Biotechnol.* **2016,** *9* (6), 758-771.
(47) Xie, Y.; Liu, Y.; Yang, J.; Liu, Y.; Hu, F.; Zhu, K.; Jiang, X. Gold Nanoclusters for Targeting Methicillin‐Resistant Staphylococcus aureus In Vivo. *Angew. Chem. Int. Ed.* **2018,** *57* (15), 3958-3962.
(48) Hagens, W. I.; Oomen, A. G.; de Jong, W. H.; Cassee, F. R.; Sips, A. J. What do we (need to) know about the kinetic properties of nanoparticles in the body? *Regul. Toxicol. Pharmacol.* **2007,** *49* (3), 217-229.
(49) Li, M.; Al-Jamal, K. T.; Kostarelos, K.; Reineke, J. Physiologically based pharmacokinetic modeling of nanoparticles. *ACS nano* **2010,** *4* (11), 6303-6317.
(50) Memarzadeh, K.; Vargas, M.; Huang, J.; Fan, J.; Allaker, R. In *Nano metallic-oxides as antimicrobials for implant coatings*, Key Eng. Mater., Trans Tech Publ: 2012; pp 489-494.
(51) Maness, P.-C.; Smolinski, S.; Blake, D. M.; Huang, Z.; Wolfrum, E. J.; Jacoby, W. A. Bactericidal activity of photocatalytic TiO2 reaction: toward an understanding of its killing mechanism. *Appl. Environ. Microbiol.* **1999,** *65* (9), 4094-4098.

(52) Allaker, R. P.; Memarzadeh, K. Nanoparticles and the control of oral infections. *Int. J. Antimicrob. Agents* **2014,** *43* (2), 95-104.
(53) Vasilache, V.; Popa, C.; Filote, C.; Cretu, M. A.; Benta, M. In *Nanoparticles applications for improving the food safety and food processing*, 7th International Conference on Materials Science and Engineering–BRAMAT Braşov, ebruary, 2011; pp 24-26.
(54) Lam, S. J.; O'Brien-Simpson, N. M.; Pantarat, N.; Sulistio, A.; Wong, E. H.; Chen, Y.-Y.; Lenzo, J. C.; Holden, J. A.; Blencowe, A.; Reynolds, E. C. Combating multidrug-resistant Gram-negative bacteria with structurally nanoengineered antimicrobial peptide polymers. *Nat. Microbiol.* **2016,** *1*, 16162.
(55) Chakraborty, D.; Chauhan, P.; Alex, S. A.; Chaudhary, S.; Ethiraj, K.; Chandrasekaran, N.; Mukherjee, A. Comprehensive study on biocorona formation on functionalized selenium nanoparticle and its biological implications. *J. Mol. Liq.* **2018,** *268*, 335-342.
(56) Li, X.; Huang, T.; Heath, D. E.; O'Brien-Simpson, N. M. O. C., Andrea J Antimicrobial nanoparticle coatings for medical implants: design challenges and prospects. *Biointerphases* **2020,** *15* (6), DOI: 10.1116/6.0000625.
(57) Tran, P. A.; O'Brien-Simpson, N.; Palmer, J. A.; Bock, N.; Reynolds, E. C.; Webster, T. J.; Deva, A.; Morrison, W. A.; O'connor, A. J. Selenium nanoparticles as anti-infective implant coatings for trauma orthopedics against methicillin-resistant Staphylococcus aureus and epidermidis: in vitro and in vivo assessment. *Int. J. Nanomedicine* **2019,** *14*, 4613.
(58) Higgins, C. F.; Hiles, I. D.; Salmond, G. P.; Gill, D. R.; Downie, J. A.; Evans, I. J.; Holland, I. B.; Gray, L.; Buckel, S. D.; Bell, A. W. A family of related ATP-binding subunits coupled to many distinct biological processes in bacteria. *Nature* **1986,** *323* (6087), 448.
(59) Applerot, G.; Lipovsky, A.; Dror, R.; Perkas, N.; Nitzan, Y.; Lubart, R.; Gedanken, A. Enhanced antibacterial activity of nanocrystalline ZnO due to increased ROS‐mediated cell injury. *Adv. Funct. Mater.* **2009,** *19* (6), 842-852.
(60) Hurdle, J. G.; O'neill, A. J.; Chopra, I.; Lee, R. E. Targeting bacterial membrane function: an underexploited mechanism for treating persistent infections. *Nat. Rev. Microbiol.* **2011,** *9* (1), 62-75.
(61) Benarroch, J. M.; Asally, M. The Microbiologist's Guide to Membrane Potential Dynamics. *Trends Microbiol.* **2020**.
(62) Chudobova, D.; Cihalova, K.; Dostalova, S.; Ruttkay-Nedecky, B.; Merlos Rodrigo, M. A.; Tmejova, K.; Kopel, P.; Nejdl, L.; Kudr, J.; Gumulec, J. Comparison of the effects of silver phosphate and selenium nanoparticles on Staphylococcus aureus growth reveals potential for selenium particles to prevent infection. *FEMS Microbiol. Lett.* **2014,** *351* (2), 195-201.
(63) Liu, W.; Golshan, N. H.; Deng, X.; Hickey, D. J.; Zeimer, K.; Li, H.; Webster, T. J. Selenium nanoparticles incorporated into titania nanotubes inhibit bacterial growth and macrophage proliferation. *Nanoscale* **2016,** *8* (34), 15783-15794.
(64) Panáček, A.; Kvítek, L.; Smékalová, M.; Večeřová, R.; Kolář, M.; Röderová, M.; Dyčka, F.; Šebela, M.; Prucek, R.; Tomanec, O. Bacterial resistance to silver nanoparticles and how to overcome it. *Nat. Nanotechnol.* **2018,** *13* (1), 65.
(65) Skalickova, S.; Milosavljevic, V.; Cihalova, K.; Horky, P.; Richtera, L.; Adam, V. Selenium nanoparticles as a nutritional supplement. *Nutrition* **2017,** *33*, 83-90.
(66) Zhao, Y.; Tian, Y.; Cui, Y.; Liu, W.; Ma, W.; Jiang, X. Small molecule-capped gold nanoparticles as potent antibacterial agents that target gram-negative bacteria. *J. Am. Chem. Soc.* **2010,** *132* (35), 12349-12356.
(67) Hinterwirth, H.; Wiedmer, S. K.; Moilanen, M.; Lehner, A.; Allmaier, G.; Waitz, T.; Lindner, W.; Lämmerhofer, M. Comparative method evaluation for size and size‐distribution analysis of gold nanoparticles. *J. Sep. Sci.* **2013,** *36* (17), 2952-2961.
(68) Shen, W.-C.; Yang, D.; Ryser, H. J.-P. Colorimetric determination of microgram quantities of polylysine by trypan blue precipitation. *Anal. Biochem.* **1984,** *142* (2), 521-524.
(69) CLSI. Methods for dilution antimicrobial susceptibility tests for bacteria that grow aerobically; Approved standard: M07-A10. *Wayne, PA: Clinical and Laboratory Standards Institute* **2015**.

(70) CLSI. Methods for determining bactericidal activity of antimicrobial agents; Approved guideline: M26-A. *Wayne, PA: Clinical and Laboratory Standards Institute* **1999**.

GRAPHIC ABSTRACT

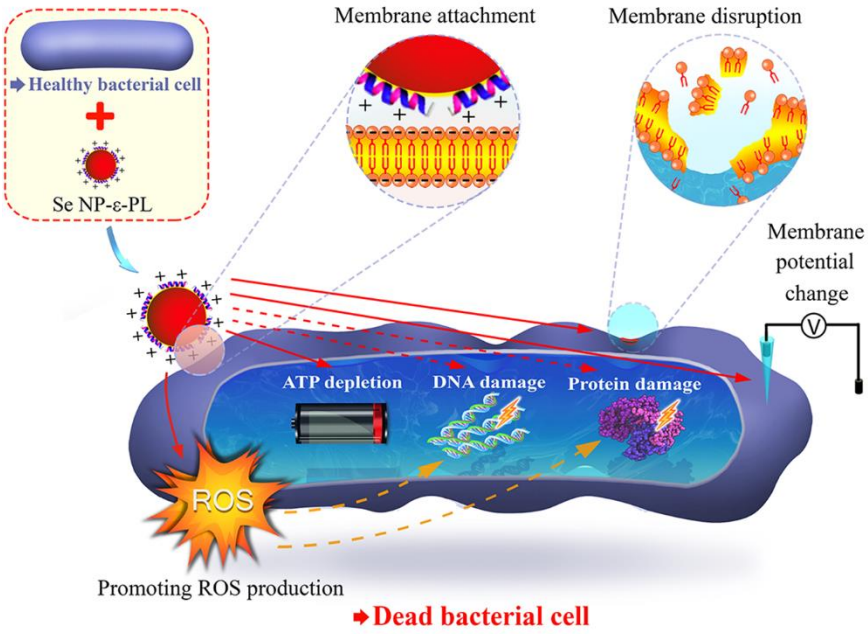
Healthy bacterial cell
Se NP-ε-PL
Membrane attachment
Membrane disruption
Membrane potential change
V
ATP depletion
DNA damage
Protein damage
ROS
Promoting ROS production
Dead bacterial cell